Analysis of Rear Seat Shoulder Belt Anchor Position on Kinematics of Small Stature Female in Frontal Impact

Patrick Thangarajah[1], Brock Watson[1], Kathy Tang[1,2], and Suzanne Tylko[2], Duane Cronin[1]
[1]University of Waterloo; [2] Innovation Center, Transport Canada

ABSTRACT

Significant advancements in vehicle safety have benefited vehicle occupants, while seat belt loading has been identified as a source of thoracic injuries, particularly for rear seat occupants. Previous studies have investigated rear seat occupant response with the THOR-50M, HIII-50M, and HIII-5F in physical tests and simulations, reporting that the shoulder belt anchor (D-ring) position affects response, with an effect of occupant stature, but have not considered the recent small stature female THOR-5F Anthropometric Test Device (ATD). The objectives of the present study were to validate a THOR-5F FE model in a simplified rigid seat environment against physical tests, and use the model to quantify the effect of seat belt D-ring position on ATD response, specifically focusing on chest compression and pelvis acceleration. Three frontal sled tests were conducted using the THOR-5F ATD on a rigid bench with an acceleration pulse taken from a full-scale vehicle-to-vehicle frontal offset crash test (23g peak acceleration). The ATD was positioned and measured with a FaroArm 3D metrology to ensure consistent positioning between tests. A THOR-5F FE model was positioned in a model of the rigid bench to match the physical tests, and respective kinematics were compared for validation. The D-ring position was then varied within the model in fore/aft (X), lateral (Y), vertical (Z) from a baseline average position, based on reported ranges. Peak chest deflections, measured at four chest IR-TRACC sensors in the left and right, lower and upper chest regions, were averaged and compared. Peak pelvis acceleration was included for insight into potential effects on lower body kinematics. The baseline position had 32 mm average peak chest deflection and 37g peak pelvis acceleration. The belt loads, chest compression and pelvis acceleration from the model closely matched the physical test results (0.71 average cross-correlation rating). Moving the D-ring inward, rearward and downward from the baseline reduced chest deflections and pelvic accelerations by -10% and -7% respectively; however, belt-neck contact occurred at the most inward D-ring positions and should be a consideration in D-ring location. Forward locations of the D-ring resulted in later engagement of the belt with the occupant. In general, moving the D-ring forward in X caused the largest pelvis X-acceleration change (+16% average increase), while the increase in chest deflection was primarily influenced by the Y position and, to a smaller extent, by changes in X and Z position. The FE model can be used in future exploratory research to investigate restraint system parameters.

*This paper is a student paper from the 20th Injury Biomechanics Symposium and is published in a special issue of SAE International Journal of Transportation Safety.
It is preliminary work, has not been peer reviewed, and should not be cited because it is a work in progress.*

INTRODUCTION

Significant advancements in vehicle safety have benefited front seat occupants, while rear seat safety has received less attention, with seatbelt interaction identified as a contributing source of thoracic injuries. A 2015 study analyzing two automotive crash databases, the National Automotive Sampling System Crashworthiness Data System (NASS-CDS) and the Fatality Analysis Reporting System (FARS), found that vehicle models newer than 2007 have a 46% higher risk of fatality for rear-seat occupants than for front-row occupants (Durbin et al., 2015; Jermakian et al., 2019). Of the reported injuries, most injured occupants were female, with 22 of 36 of NASS serious (AIS 3+) injuries and 61 of the 81 FARS fatalities. The lower safety for rear-seat occupants compared to the front seat has resulted in a heightened focus on rear seat safety (Beck et al., 2016).

Seatbelts, particularly the shoulder belts, were identified as the most common source of injuries, leading to chest and abdominal trauma (Beck et al., 2016; Jermakian et al., 2019). A 2019 study found that serious chest injuries occurred in 22 out of 36 injured occupants and were attributed to shoulder belt loading. The absence of airbags and seatbelt technologies, such as pre-tensioners and load limiters, in the rear seat has potentially resulted in a higher influence of belt anchor location on injury, with the shoulder belt anchor (D-ring) position affecting the upper body kinematics of rear seat occupants (Meng et al., 2025; Youn et al., 2015).

A study conducted in 2022 utilized physical frontal impact sled tests to assess the influence of the D-ring vertical position on the sternum deflection in the HIII 5th percentile (HIII-5F) Anthropometric Testing Device (ATD), finding that higher vertical positions resulted in lower sternum deflections (Edwards et al., 2022). Additionally, several studies have investigated the effects of D-ring locations on rear-seat kinematics using various finite element (FE) models of ATDs. The models in these studies include the Hybrid III 50th percentile male (H-III 50M), the Test Device for Human Occupant Restraint M50 (THOR-50M), and the HIII-5F (Hu et al., 2013; Meng et al., 2025; Youn et al., 2015). Findings indicated that the X position of the D-ring largely affected kinematics such as chest deflection and head injury, with varying optimal D-ring locations based on ATD model stature (Hu et al., 2013; Meng et al., 2025; Youn et al., 2015). The past studies have not considered the THOR 5th percentile ATD (THOR-5F), the contemporary replacement of the currently used HIII 5th percentile ATD with improved biofidelity (Wang et al., 2018).

The present study aimed to investigate the effect of shoulder belt D-ring location on chest and pelvis kinematics using a contemporary ATD. The first step was to test the THOR-5F in a rigid bench configuration based on measurements from rear seats in the automotive fleet. Then, a THOR-5F FE model (ATD Models GmbH, Germany) was validated with the experimental data. Next, a parametric study was undertaken to assess the influence of the D-ring location on the chest and pelvis kinematics of the THOR-5F FE model. The results were assessed in terms of sensitivity or changes in response with varying D-ring position.

This paper is a student paper from the 20th Injury Biomechanics Symposium and is published in a special issue of SAE International Journal of Transportation Safety.
It is preliminary work, has not been peer reviewed, and should not be cited because it is a work in progress.

METHODS

Validation of THOR-5F FE model in sled with rigid bench

Physical rigid bench testing. Physical sled testing was conducted in a setup consisting of a sled base and a mounted rigid bench, which included a seat pan, seatback, retractor, D-ring, lap belt anchors, and a raised platform to offset the seated THOR-5F from the lap belt anchors (Figure 1**Error! Reference source not found.**). The D-ring location was based on the FMVSS 213 sled, intended to represent an average rear seat (Aram & Rockwell, 2012).

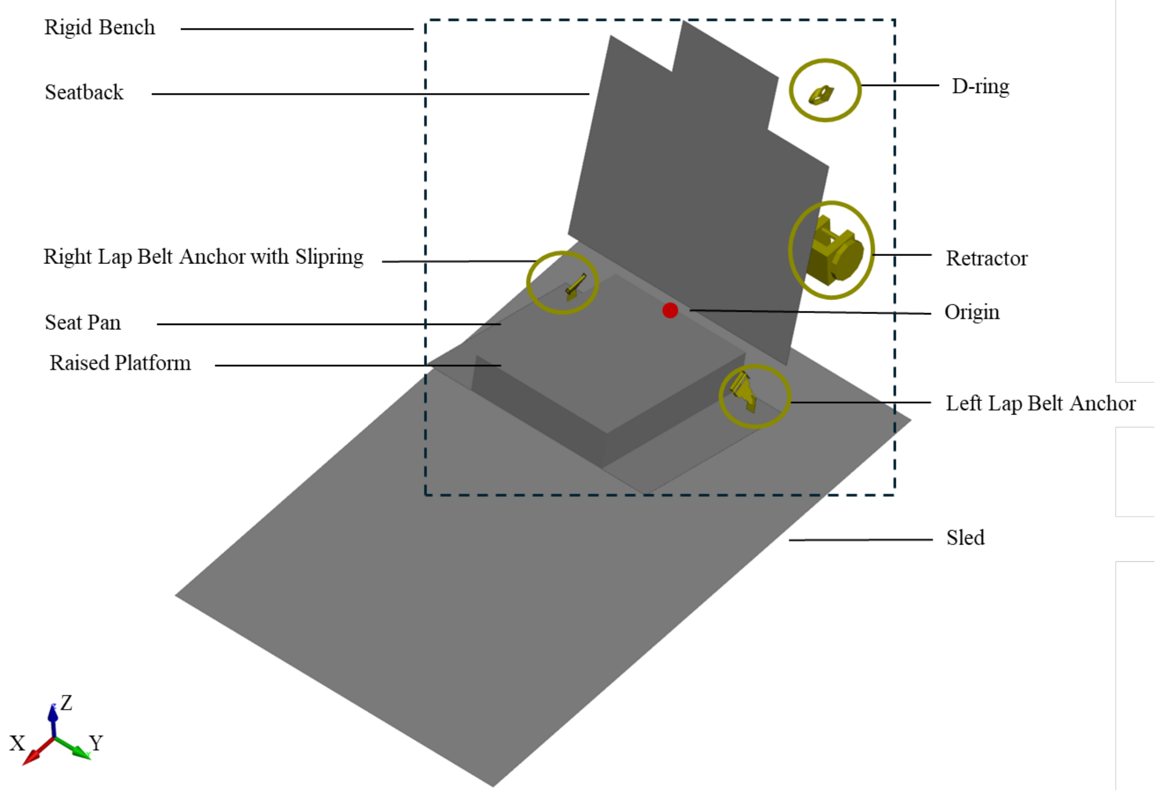

Figure 1: FE model of sled with rigid bench. The origin (red dot) is X, Y, Z = (0,0,0).

Three sled tests were conducted with the THOR-5F installed on the rigid bench (Figure 2A) and subjected to a 23g peak acceleration crash pulse (Figure 2B), taken from measurements at the center of gravity of a vehicle in a frontal offset vehicle-vehicle crash test. For each test, the THOR-5F physical ATD (Humanetics) was consistently positioned, confirmed by 3D scans and FaroArm 3D measurements within 18 mm of each other (Table 1). The belt anchor locations were consistent for all tests.

This paper is a student paper from the 20th Injury Biomechanics Symposium and is published in a special issue of SAE International Journal of Transportation Safety.
It is preliminary work, has not been peer reviewed, and should not be cited because it is a work in progress.

A B
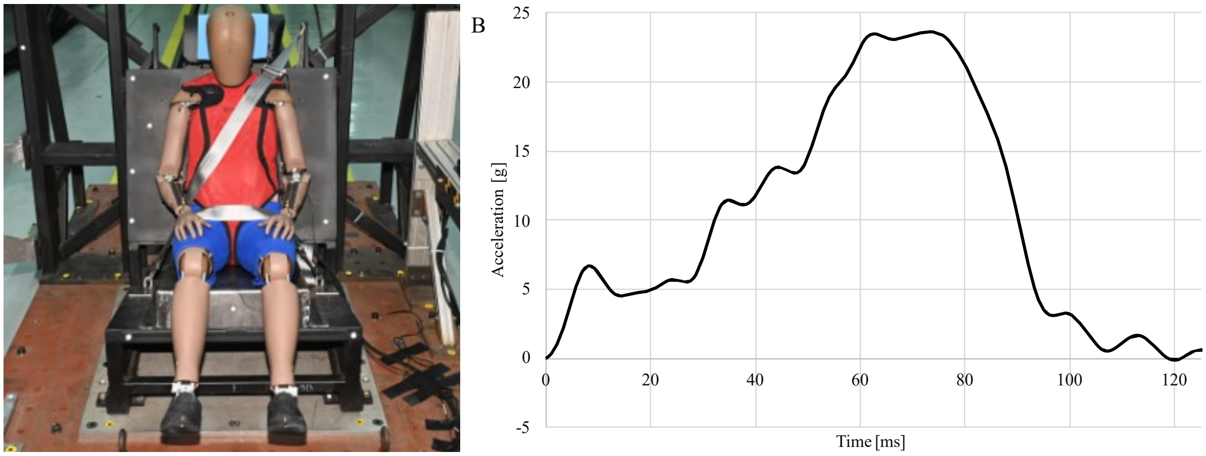

Figure 2: (A) Physical rigid bench test setup with THOR-5F and (B) sled acceleration pulse used in physical tests

Table 1: Maximum difference between FaroArm measurements for ATD positioning landmarks

Faro measurement	**Maximum difference between test positions (mm)**		
	X	**Y**	**Z**
Head target sticker, right side	3	4	4
H-Point, on tool, right side	5	3	9
Left knee, interior side	1	1	5
Left ankle front bolt, center of the bolt head	2	18	4
Heel of left foot	9	14	11
Left toe, foremost point	5	6	14
Right knee, exterior side	6	4	5
Right ankle front bolt, center of the bolt head	3	6	2
Heel of right foot	6	8	4
Right toe, foremost point	6	5	5
Glabella (Nose, at the top between the eyes)	6	2	3
Chin center	2	1	0
Yaw reference point, right side	6	0	4
Shoulder belt, upper edge, at y=0	3	1	6
Shoulder belt, lower edge, at y=0	2	1	6
Lap belt, upper edge, at y=0	3	0	2
Lap belt, lower edge, at y=0	3	1	4
Shoulder front bolt, left shoulder, center of the head or tail of the bolt	9	5	3
Left arm exterior elbow bolt, center of the bolt head	3	5	4
Left arm wrist interior bolt, center of the bolt head	2	5	4
Shoulder front bolt, right shoulder, center of the head or tail of the bolt	1	4	4
Right arm exterior elbow bolt, center of the bolt head	3	3	3
Right arm wrist interior bolt, center of the bolt head	1	1	3

FE model of sled and rigid bench. A model of the physical sled and rigid bench was created using detailed geometry and steel material properties (Figure 1). The D-ring and lap belt anchors were positioned in the baseline position, with locations matching the physical rigid bench (Table 2). The belt system integrated into the rigid bench model used the geometry and material properties from an open source seat belt model (Eggers et al., 2023), with the retractor pullout updated to match data from the Transport Canada retractor used in the study (Figure 3). Belt slack was removed by the retractor to achieve the measured belt tension at the start of the physical sled test.

Table 2: Spatial coordinates of belt anchors in baseline position

Anchor	X (mm)	Y (mm)	Z (mm)
D-ring position	-316.9	262.0	699.0
Right lap belt anchor	45.2	-286.6	-62.0
Left belt anchor	45.2	286.6	-62.0

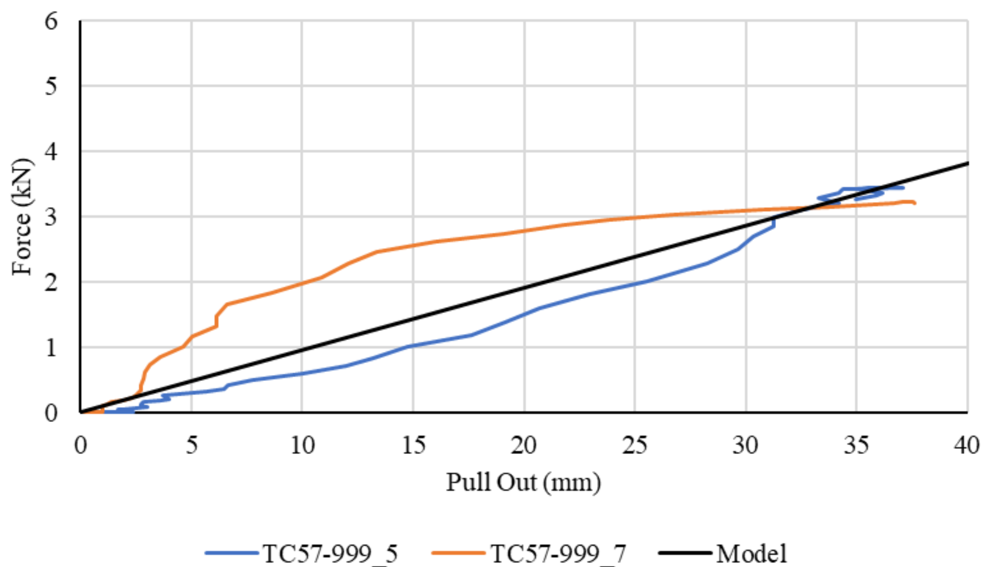

Figure 3: Retractor force vs pullout test data from TC (orange and blue) and adjusted retractor vs pullout data implemented in TC rigid bench model.

Positioning of THOR-5F FE model in rigid bench FE model. The first step in validating the THOR-5F FE model involved positioning the model to match the physical ATD starting position. A wireframe was generated from the average FaroArm measurements of the test positions (Figure 4A). The THOR-5F FE model was then manually positioned using LS-PrePost V4.10 to align with the wireframe at 18 locations (Figure 4B), and further refined by overlaying the 3D scan of the physical THOR-5F ATD test position on the model (Figure 4C) and adjusting limb positions to align with the scan. The THOR-5F FE model position was then saved as a target position. Next, a pre-simulation applied a "marionette"(Asadi & Karlsson, 2023) positioning approach where tensioned cables pulled the model to the target position without causing interference between close-fitting parts (Figure 5).

This paper is a student paper from the 20th Injury Biomechanics Symposium and is published in a special issue of SAE International Journal of Transportation Safety.
It is preliminary work, has not been peer reviewed, and should not be cited because it is a work in progress.

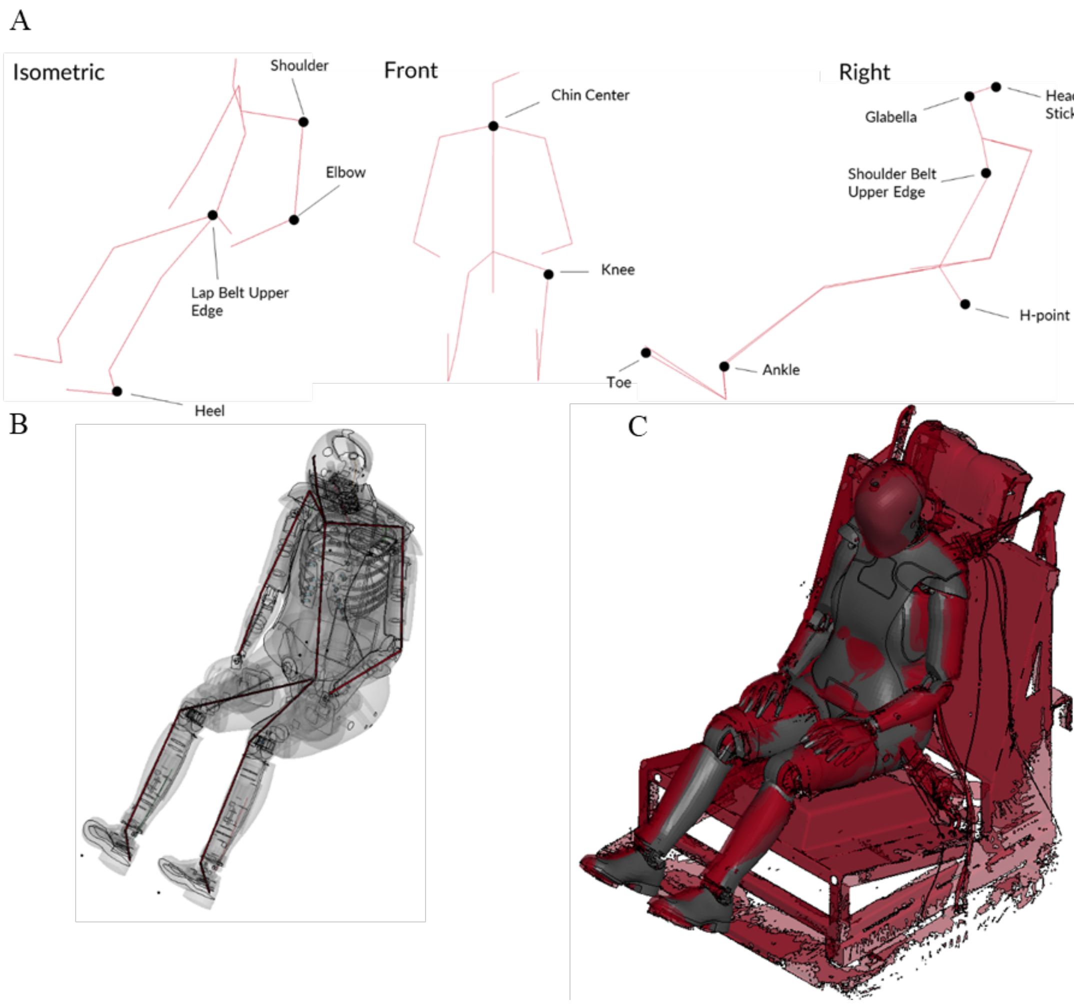

Figure 4: (A) Wireframe from average of FaroArm measurements of physical THOR-5F ATD position used for positioning THOR-5F FE model, (B) Overlay of wireframe (red) on positioned THOR-5F FE model (gray), (C) Overlay of the THOR-5F FE model (gray) and the 3D scan of physical THOR-5F ATD (red).

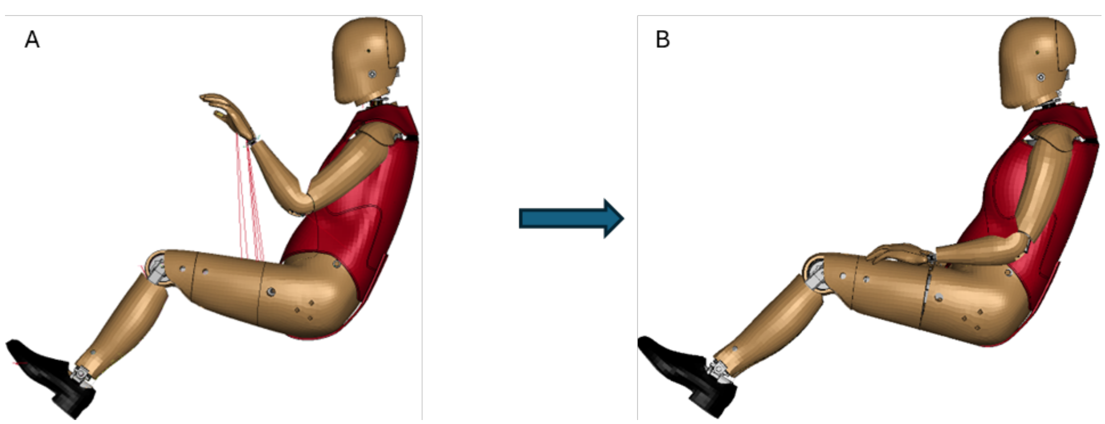

Figure 5: Overview of the positioning pre-simulation, where cables moved the THOR-05F FE model from a (A) start position to a (B) target position.

After positioning, the open-source belt model was integrated and routed around the THOR-5F FE. Finally, the 23g crash acceleration pulse (Figure 2B) was applied to the sled. The model was solved using LS-DYNA (R12.2.1, MPP, single precision) on a parallel computing platform (32 CPUs). The following ATD measurements were used for comparison to the test: head X-acceleration, 1D chest sensor deflections, pelvis X-acceleration, belt loads.

Varying D-ring simulations with THOR-5F FE model

In addition to the baseline model, eight simulations were run with the D-ring positioned at combinations of maximums and minimums in X (fore-aft), Y (lateral), Z (vertical) locations (Figure 6), to determine the effect of D-ring location on THOR-5F kinematics in the rigid bench. The maximum and minimum locations were from a study that measured the X, Y, Z distances from the D-ring to a fixed reference point for 24 vehicles, including multi-purpose vehicles, passenger cars, and trucks (Aram & Rockwell, 2012). These measurements provided maximum and minimum D-ring locations to evaluate sensitivity to D-ring placement.

Position	X	Y	Z
1	Baseline	Baseline	Baseline
2	Minimum	Maximum	Maximum
3	Minimum	Minimum	Minimum
4	Maximum	Minimum	Maximum
5	Maximum	Maximum	Maximum
6	Minimum	Minimum	Minimum
7	Maximum	Minimum	Minimum
8	Maximum	Maximum	Minimum
9	Minimum	Maximum	Minimum

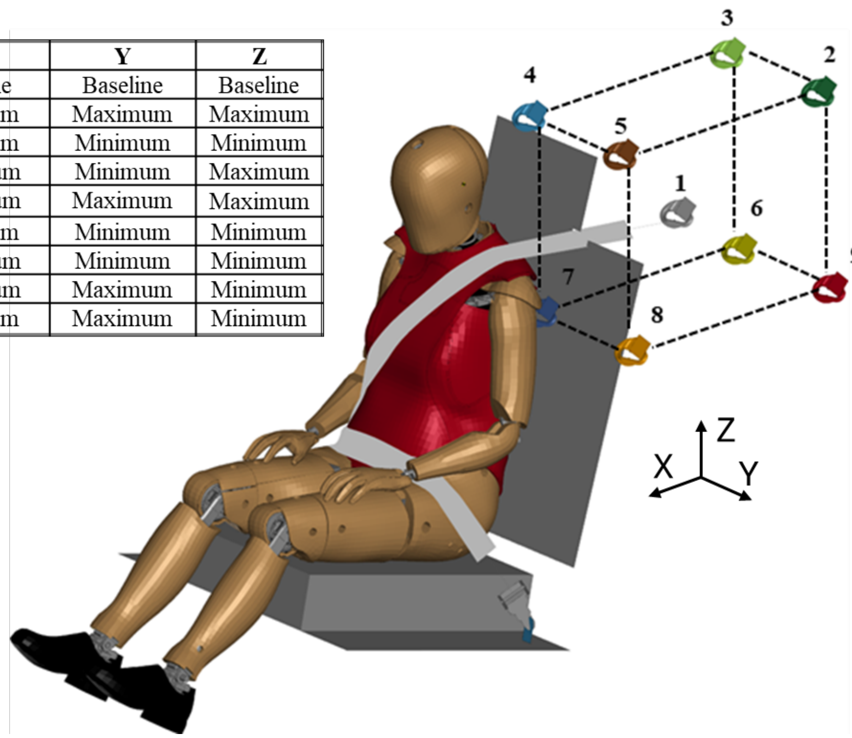

Figure 6: D-ring positions investigated based on reported maximum and minimum measurements from Aram & Rockwell (2012). Baseline model (Position 1) belt routing shown in gray.

After setting the D-ring location, the THOR-5F FE model was belted using LS-PrePost V4.10 and simulated with the 23g crash pulse. The kinematic measurements investigated were the peak sensor deflection at each of the four 1D chest sensors (upper right, upper left, lower right, lower left) and the pelvis X-acceleration, as the motion of the ATD was primarily in the forward

(X) direction. The peak chest deflection was examined due to its role as an injury assessment metric in crash tests, while pelvis X-accelerations were used to compare the lower body kinematics. From simulating Positions 2-9, the main effects were calculated using the standard Design of Experiments approach ((Equation 1), where input variables were modified to analyze their impact on a response (Durakovic, 2017)The main effects of peak chest deflection were calculated using the average peak deflection of all four IR-TRACC sensors.

$$\text{Main Effect}_{x,y,z} = \mu(\text{Maximum Positions}) - \mu(\text{Minimum Positions}) \qquad \text{(Equation 1)}$$

RESULTS

Validation of THOR-5F FE model in sled with rigid bench

After simulating the baseline configuration (D-Ring Position 1), the kinematic traces were compared with the physical test results. The shoulder belt force, lap belt force, and pelvis acceleration of the THOR-5F FE model had similar magnitude and timing as the THOR-5F physical ATD, showing accurate belt interaction of the model and lower body kinematics. The upper body motion differed between the simulation and the experiments, particularly in the head kinematics (Figure 7A), which experienced nearly 3 times higher peak accelerations. The deflections of the chest regions in the model generally matched with test results, with peak deflections ranging from 0.86 to 1.14 times the physical test traces (Figure 7B,D,E). However, the peak deflection of the left lower chest (Figure 7C) was 0.44 times the average physical test deflection.

This paper is a student paper from the 20th Injury Biomechanics Symposium and is published in a special issue of SAE International Journal of Transportation Safety. It is preliminary work, has not been peer reviewed, and should not be cited because it is a work in progress.

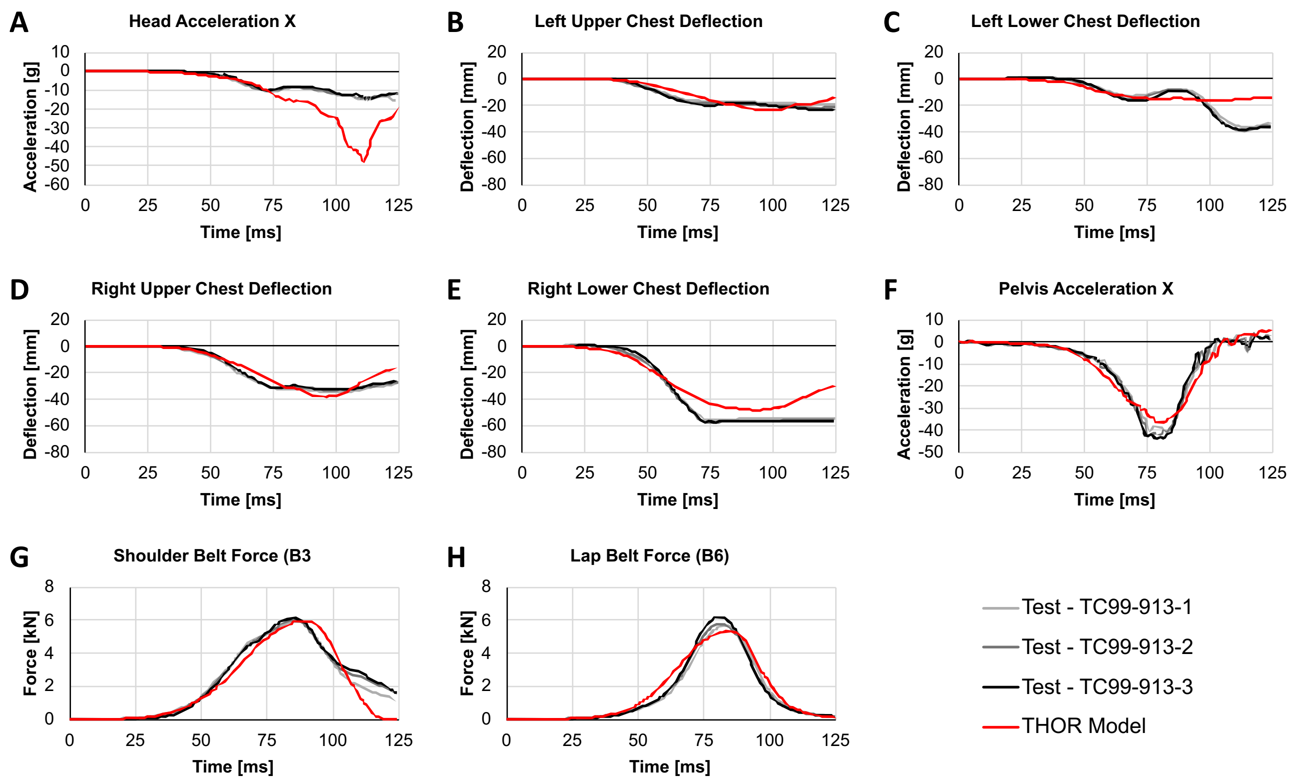

Figure 7: Responses of THOR-5F FE model compared to the physical THOR-5F ATD in the rigid bench.

For a quantitative comparison between the THOR-5F FE model and the physical ATD, ARCGen (Hartlen & Cronin, 2022), was used to calculate a cross-correlation rating according to ISO18571 without using the corridor rating and evaluating magnitude, phase and slope. The correlation rating can range from 0 to 1, with 1 indicating excellent correlation and 0 denoting poor correlation. The cross-correlation ratings for the model compared to the experiments ranged from 0.31 for head X-acceleration to 0.92 for lap belt load (Table 3), with an overall average of 0.71, indicating fair correlation between the model and physical ATD kinematics.

Table 3: Cross Correlation Ratings of the THOR-5F FE model and THOR-5F physical ATD in rigid bench tests (ISO 18571 method)

Response	Cross-correlation rating
Head X-acceleration	0.31
Chest left lower deflection	0.55
Chest left upper deflection	0.61
Chest right lower deflection	0.74
Chest right upper deflection	0.80
Pelvis X-acceleration	0.87
Shoulder belt load	0.87
Lap belt load	0.92
Average	0.71

*This paper is a student paper from the 20th Injury Biomechanics Symposium and is published in a special issue of SAE International Journal of Transportation Safety.
It is preliminary work, has not been peer reviewed, and should not be cited because it is a work in progress.*

Effect of D-ring location on kinematics of small statured female

Across all D-ring positions, the average peak chest deflections ranged from 11 to 40 mm (Figure 8A). In most D-ring positions, the right lower chest experienced the highest peak deflection, while the left lower chest had the lowest deflection. The peak pelvis X-acceleration ranged from -34 g to -56 g (Figure 8B), with Position 8 (X_{min}, Y_{max}, Z_{min}) resulting in the highest acceleration and Position 6 (X_{max}, Y_{min}, Z_{min}) resulting in the lowest acceleration. Position 8 resulted in the belt slipping from the THOR-5F FE shoulder to below the chest and was excluded from further analysis and discussion. The cause of belt migration will be investigated in future studies.

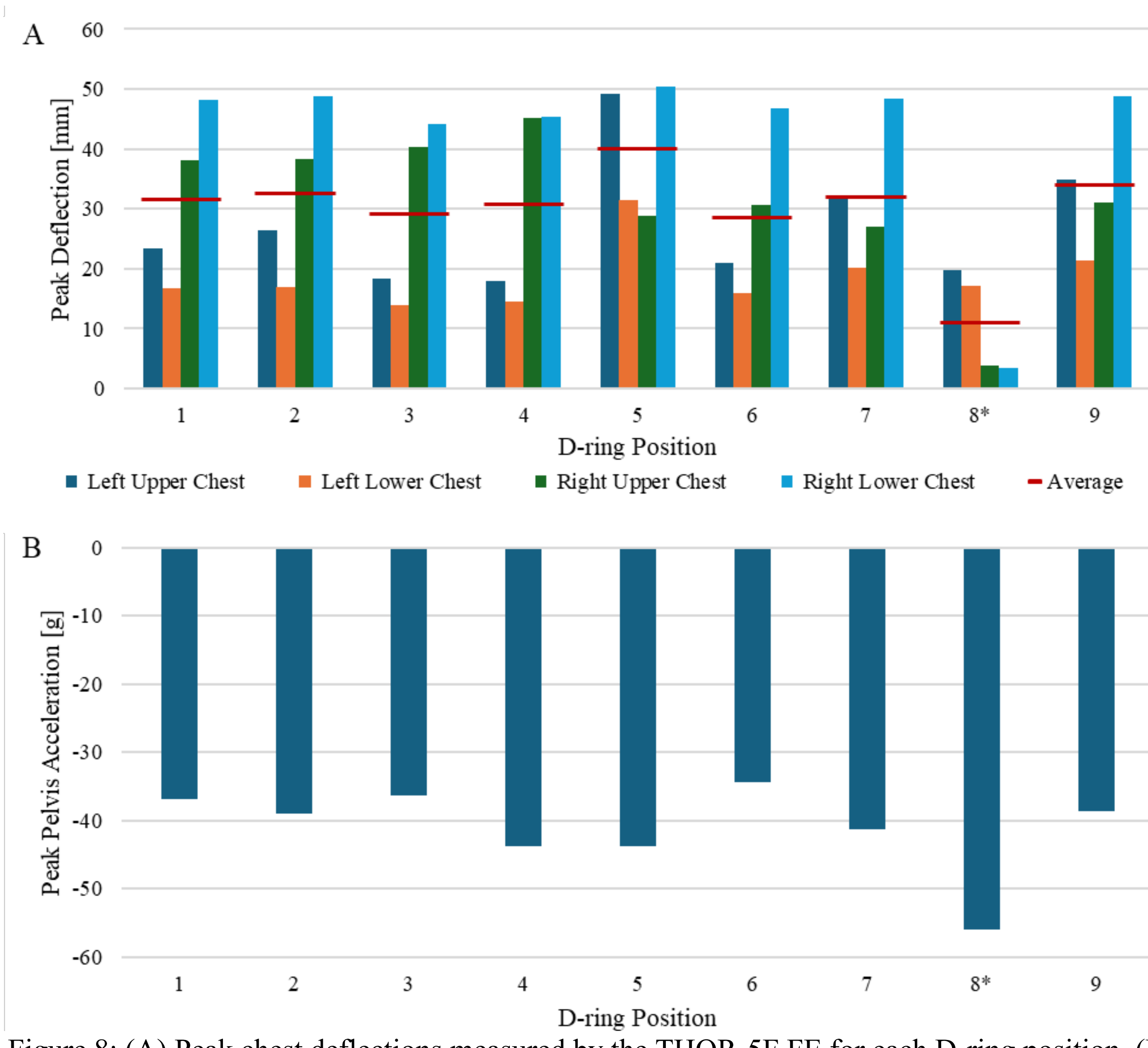

Figure 8: (A) Peak chest deflections measured by the THOR-5F FE for each D-ring position. (B) Peak pelvis X-accelerations measured by the THOR-5F FE for each D-ring position. *Position 8 resulted in belt slippage, causing low chest deflections and high pelvis X-accelerations, and was removed from the analysis.

This paper is a student paper from the 20th Injury Biomechanics Symposium and is published in a special issue of SAE International Journal of Transportation Safety. It is preliminary work, has not been peer reviewed, and should not be cited because it is a work in progress.

The average peak chest deflection measured in the baseline position was 32 mm, with a peak pelvis X-acceleration of -37 g. Position 5 (X_{min}, Y_{max}, Z_{max}) showed increases in pelvis X-acceleration (19%) and chest deflection (26%). The other positions recorded lower average peak chest deflections than baseline, with Positions 3 (X_{max}, Y_{min}, Z_{max}) and 6 resulting in the largest decreases (-8% for Position 3, -10% for Position 6). Additionally, peak pelvis X-accelerations were lower than the baseline when the D-ring was at Positions 3 (-2%) and 6 (-7%). On average, forward D-ring locations resulted in a 16% increase in pelvis X-acceleration relative to baseline.

The main effects calculations indicated that the D-ring Y-position substantially influenced the average peak chest deflection; increasing the D-ring Y-position from minimum to maximum (e.g. Position 4 to 5) increased average peak chest deflection by 5.9 mm (Figure 9). The X and Z-positions of the D-ring also affected chest deflection; increasing the X-position (e.g. Position 2 to 5) caused an increase of 3.1 mm. In comparison, increasing the Z-position (e.g. Position 8 to 5) caused a 1.6 mm increase in chest deflection. The primary effect on peak pelvis X-acceleration was attributed to the D-ring X-position, as increasing the X-position resulted in a 5.9 g increase in peak pelvis X-acceleration magnitude. The primary effects of the Y and Z-positions were lower, with Z-position elevation resulting in a 2.6 g increase in peak pelvis X-acceleration magnitude, and a 1.5 g increase when increasing the Y-position outboard.

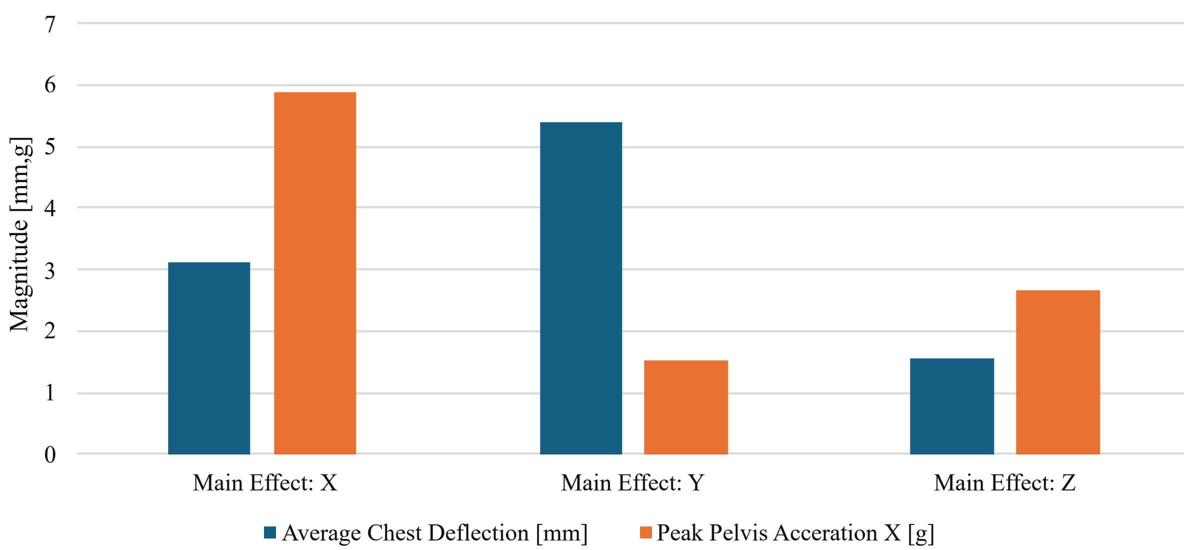

Figure 9: Main effect magnitude of D-ring position on chest compression and pelvis X-acceleration measured by the THOR-5F FE model.

This paper is a student paper from the 20th Injury Biomechanics Symposium and is published in a special issue of SAE International Journal of Transportation Safety.
It is preliminary work, has not been peer reviewed, and should not be cited because it is a work in progress.

DISCUSSION

Validation of THOR-5F FE model in sled with rigid bench

The validation of the THOR-5F FE model showed good agreement with the physical ATD for belt loads, chest deflections and pelvis accelerations, demonstrating close alignment between the THOR-5F FE model and physical ATD in bench and belt interactions. While the kinematics were generally consistent between the model and physical ATD, differences were observed at maximum excursion (105 ms). In the physical test, the shoulder belt migrated laterally outwards on the shoulder of the THOR-5F ATD, and the torso rotated about the Z-axis with minimal pelvis rotation (Figure 8A,B), which was not replicated in the model (Figure 10C,D). The lack of torso Z-rotation in the model resulted in abrupt loading at the end of the excursion, leading to higher head X-accelerations and left upper chest deflections. The lower torso rotation in the FE model was investigated by reviewing the baseline model, and in a separate study with varying belt routing and occupant initial position. No substantial changes to the kinematics were observed when varying belt routing and initial position. It is hypothesized that the reduced torso rotation in the model may stem from a higher Z-rotation stiffness, potentially in the lumbar spine in the model, and is a topic for further investigation. However, the close match between the FE model and the physical ATD in the regions of interest (belt loads, thoracic deflection, and pelvis X-acceleration) and at earlier time points than shown in Figure 10 indicated that the model could provide guidance on the effect of D-ring positions.

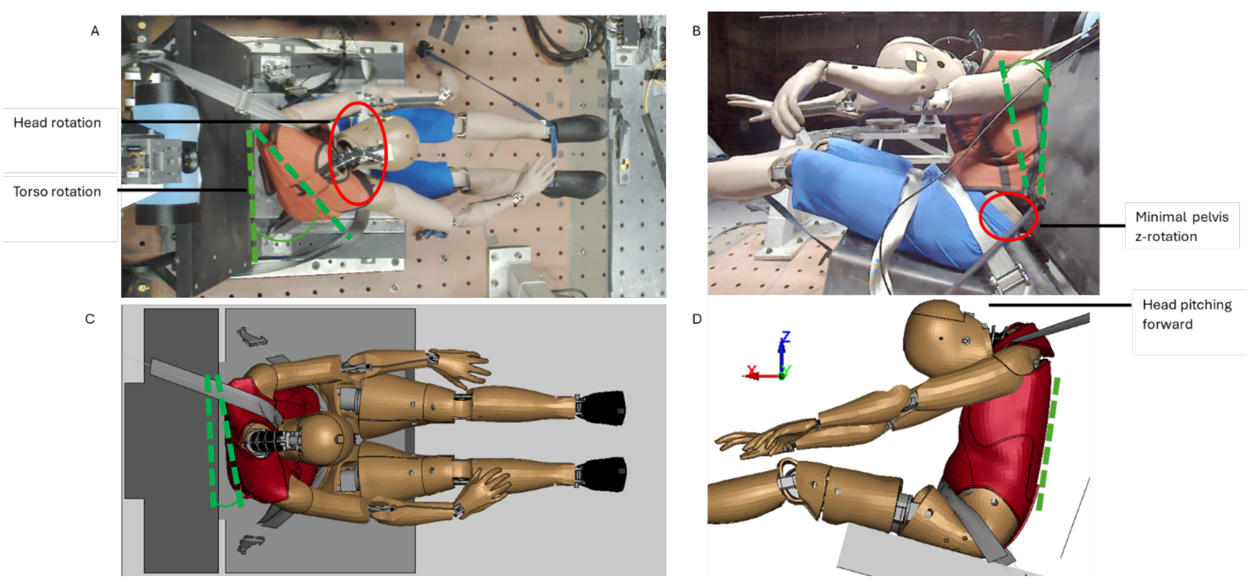

Figure 10: THOR-5F at 105 ms, (A) Top view of physical ATD, (B) Side view of physical ATD, (C) Top view of FE model (D) Side view of FE model. The reduced torso rotation of the THOR-5F FE model, shown by the angle indicator (dashed green lines), resulted in higher head accelerations at the end of the crash pulse.

This paper is a student paper from the 20th Injury Biomechanics Symposium and is published in a special issue of SAE International Journal of Transportation Safety.
It is preliminary work, has not been peer reviewed, and should not be cited because it is a work in progress.

Effect of D-ring location on kinematics of small stature female

The largest chest deflection and pelvis X-acceleration of the THOR-5F FE were observed when the D-ring was in Position 5 (X_{min}, Y_{max}, Z_{max}), as the shoulder belt was positioned forward relative to the THOR-5F FE model and only engaged with the thorax after the model substantially translated forward.

The main effects calculations of the pelvis X-acceleration magnitude indicated that rearward D-ring X-positions (e.g. Position 2) significantly reduced forward motion of the THOR-5F FE due to earlier belt engagement. The D-ring Y and Z-positions exhibited opposing effects, though to a lesser extent. The reduction in pelvis X-acceleration from rearward D-ring positions may also explain the lower average peak deflections associated with rearward D-ring position. However, increasing the D-ring Y-position substantially increased average peak chest deflection by altering the belt contact across the chest and shoulder. For example, in Position 9, the belt slipped outwards on the THOR-5F shoulder, resulting in higher belt loads on the chest. Increases in the Z-position had a similar but lesser effect. Various combinations of D-Ring X, Y, Z positions considerably affected peak average chest deflections; it is recommended that future studies should investigate the interactions between these effects. From the configurations considered in this study, a rearward D-ring position, while also being lower and closer inboard, reduced average peak chest deflection and pelvis X-acceleration following generally accepted optimal restraint guidelines (Eppinger, 2002). An important consideration in moving the belt inboard is the potential for interaction with the neck and neck loading from the belt, which could result in more severe injuries. While most D-ring positions followed belt design principles, some minimum Y-position D-ring configurations led to loading on the neck in this study.

Limitations

There were some limitations in the current study. While not significantly affecting the parameters of interest in the present study, the THOR-5F FE model demonstrated lower thorax Z-rotation relative to the physical ATD. A second limitation was that the D-ring positions represented maximum and minimum locations reported in the literature, and specific combinations considered may not represent contemporary vehicle mounting locations. For example, Positions 7 and 8 were outside the X and Z limits of the Canadian and Federal Motor Vehicle Safety Standards (CMVSS/FMVSS 210) (Transport Canada, n.d.; U.S. Department of Transportation, n.d.). Future research will examine D-ring locations between the maximum and minimum, corresponding to specific vehicle configurations, to further quantify the effect of D-ring location on the response of the small-stature female, with an additional focus on head and neck kinematics.

CONCLUSIONS

The validation process in this study found a generally good correspondence between the THOR-5F FE model and the THOR-5F physical ATD regarding belt loads, chest deflections, and pelvis X-accelerations. Lower torso Z-rotation of the FE model relative to the physical test was observed at the end of the impact phase and identified as a limitation of the FE model.

Considering the range of rear seat D-ring positions reported in the literature, a study on D-ring position demonstrated that shifting the belt anchor rearward and laterally inward decreased chest deflection and pelvis X-acceleration relative to the average or baseline case for the small-stature female model used in this study. Inboard positions may lead to belt interaction with the neck, and was identified by belt-neck contact for the innermost D-ring positions in this study.

The maximum and minimum D-ring positions considered in this study generally resulted in a belt fit that aligned with widely accepted paradigms, although some inboard belt configurations resulted in loading soft tissues. The position with the highest (Z), furthest forward (X), and outboard (Y) D-ring location had the largest difference from baseline (+26% chest deflection, +19% pelvis acceleration), as the forward position of the D-ring resulted in late engagement of the belt with the ATD.

Rearward D-ring positioning resulted in the largest pelvis X-acceleration decrease, while chest deflections were primarily increased by moving Y-position outwards and, to a lesser extent, by decreases in X-position and increases in Z-position. Future studies can use the THOR-5F FE model to investigate vehicle-specific D-ring locations and interaction effects for the small-stature female ATD.

ACKNOWLEDGEMENTS

The authors acknowledge Transport Canada for their financial support, ATD models GmbH for providing the computational model, and the Digital Research Alliance of Canada for providing necessary computing resources.

REFERENCES

Aram, M., & Rockwell, T. (2012). Vehicle rear seat study. *Washington (DC): National Highway Traffic Safety Administration, US Department of Transportation*.

Asadi, K., & Karlsson, K. (2023). *Automation of ATD positioning for crash analysis simulation*.

Beck, B., Bilston, L. E., & Brown, J. (2016). Injury patterns of rear seat occupants in frontal impact: An in-depth crash investigation study. *Injury Prevention: Journal of the International Society for Child and Adolescent Injury Prevention*, *22*(3), 165–170. https://doi.org/10.1136/injuryprev-2015-041715

Durakovic, B. (2017). Design of experiments application, concepts, examples: State of the art. *Periodicals of Engineering and Natural Sciences*, *5*(3), 421–439.

Durbin, D. R., Jermakian, J. S., Kallan, M. J., McCartt, A. T., Arbogast, K. B., Zonfrillo, M. R., & Myers, R. K. (2015). Rear seat safety: Variation in protection by occupant, crash and vehicle characteristics. *Accident Analysis & Prevention*, *80*, 185–192. https://doi.org/10.1016/j.aap.2015.04.006

Edwards, M. A., Jagtap, S. R., & Jermakian, J. S. (2022). Sensitivity of Established and Alternative Rear Occupant Thoracic Injury Metrics to Seat Belt Design Variables in Frontal Impacts. *Proceedings of the International Research Council on the Biomechanics on Injury, Porto, Portugal*.

Eggers, A., Schießler, M., Ott, J., Lebarbé, M., López Valdésc Manuel Valdano, F., Petit, P., Marshall, W., Lemmen, P., Östling, M., Masuda, M., Richard, O., & Beillas, P. (2023). The ENOP project (Enable New Occupant Seating Positions). In VDI Wissensforum GmbH (Ed.), *Fahrzeugsicherheit* (pp. 159–176). VDI Verlag. https://doi.org/10.51202/9783181024263-159

Eppinger, R. (2002). Occupant Restraint Systems. In A. M. Nahum & J. W. Melvin (Eds.), *Accidental Injury: Biomechanics and Prevention* (pp. 187–197). Springer New York. https://doi.org/10.1007/978-0-387-21787-1_8

Hartlen, D. C., & Cronin, D. S. (2022). Arc-length re-parametrization and signal registration to determine a characteristic average and statistical response corridors of biomechanical data. *Frontiers in Bioengineering and Biotechnology*, *10*, 843148.

Hu, J., Wu, J., Reed, M. P., Klinich, K. D., & Cao, L. (2013). Rear seat restraint system optimization for older children in frontal crashes. *Traffic Injury Prevention*, *14*(6), 614–622.

Jermakian, J., Edwards, M., Fein, S., & Maltese, M. R. (2019). Factors contributing to serious and fatal injuries in belted rear seat occupants in frontal crashes. *Traffic Injury Prevention*, *20*(sup1), S84–S91. https://doi.org/10.1080/15389588.2019.1601182

Meng, Y., Yates, K., Dahiya, A., & Untaroiu, C. D. (2025). Effects of rear seat design on occupant injury risk during frontal crashes: A parametric study using finite element analysis. *Mechanics Based Design of Structures and Machines*, *53*(1), 753–769.

Transport Canada. (n.d.). *Canada Motor Vehicle Safety Standard (CMVSS) No. 210 – Seat Belt Anchorages*. Government of Canada. https://tc.canada.ca/en/corporate-services/acts-regulations/list-regulations/motor-vehicle-safety-regulations-crc-c-1038

National Highway Traffic Safety Administration. (2020). *Federal Motor Vehicle Safety Standard No. 210 – Seat Belt Assembly Anchorages*. U.S. Department of Transportation. https://www.ecfr.gov/current/title-49/subtitle-B/chapter-V/part-571

Wang, Z. J., Lee, E., Bolte IV, J., Below, J., Loeber, B., Ramachandra, R., Greenlees, B., & Guck, D. (2018). *Biofidelity evaluation of THOR 5th percentile female ATD*. Proceedings of IRCOBI conference.

Youn, Y., Kim, H., Park, J., Lee, J., & Kim, S. (2015). Investigation of rear seat occupant potential injury risk base on seat belt configurations. *In 24th International Technical Conference on the Enhanced Safety of Vehicles (ESV) National Highway Traffic Safety Administration, 15–0443*.